Solid State Phenomena
ISSN: 1662-9779, Vol. 375, pp 13-20
doi:10.4028/p-kLR0jq

Submitted: 2024-09-19
Revised: 2025-05-06
Accepted: 2025-05-06
Online: 2025-09-05

Demonstration of Suppressing 1SSF Expansion Using Energy Filtered Ion Implantation

Hitesh Jayaprakash[1,2,4,a*], Constantin Csato[1,b], Masashi Kato[3,c], Li Tong[3,d], Florian Krippendorf[1,e], Michael Rueb[1,2,f]

[1]mi2-factory GmbH, Moritz-von-Rohr Str. 1a, 07745 Jena, Germany

[2]Ernst Abbe Hochschule, Carl-Zeiss-Promenade 2, 07745 Jena, Germany

[3]Nagoya Institute of Technology, Gokiso, Showa, Nagoya 466-8555, Japan

[4]Friedrich Alexander Universität, Cauerstr. 6, 91058 Erlangen, Germany

[a]hitesh.jayaprakash@eah-jena.de, [b]constantin.csato@mi2-factory.com, [c]kato.masashi@nitech.ac.jp, [d]li.tong@nitech.ac.jp, [e]florian.krippendorf@mi2-factory.com, [f]michael.rueb@mi2-factory.com

Keywords: 1SSF, BPD, Bipolar degradation, Ion Implantation, Carrier Lifetime

Abstract. Bipolar degradation poses a significant concern for the reliability of SiC bipolar power devices. The basic cause for bipolar degradation is expansion of Shockley Stacking Faults SSFs. These glide planes can be pinned and prevented from expansion. This study involves 19 MeV Energy Filtered Ion Implantation of Nitrogen (i.e. resulting in an energy spectrum ranging from 0 MeV to nearly 19 MeV in one shot) to explore the pinning effect of Nitrogen ions that suppresses recombination glide, which minimizes SSF growth, while providing precise doping of the entire drift region by the same Nitrogen implantation. All is performed in one single step. This procedure paves the path to immobilize any nucleation sites in the entire drift layer, this way enhancing the reliability and facilitating mass production of SiC power devices. This study employs UV illumination as an optical stressing method to create e-/h+ pair, which subsequently induce 1SSF expansion. Both, UV induced 1SSF expansion and pining were observed by photoluminescence. Carrier lifetime measurements were employed for understanding the mechanism of pinning defects.

Introduction

In recent years, there has been an increase in demand for 4H-SiC wide band gap semiconductor for power device manufacturing [1], in particular to its superior physical properties that outperform conventional silicon for high voltage and high current device applications [2]. The power devices that are fabricated from 4H-SiC suffer from several potential reliability issues [3–6]. These issues arise from material defects, gate-oxide reliability and other process related defects. Bipolar degradation as another very critical reliability mechanism is caused by material defects [7] under bipolar (electron hole plasma) current stress. Mitigation of this degradation effect can significantly improve the overall reliability of the SiC power devices.

The expansion of 1SSF by the mechanism of recombination enhanced dislocation glide (REDG) is considered to be the root cause and has been well understood in the recent decade [8–12]. The earliest approaches on pinning glide planes with ion implantation demonstrated that the material defects are pinned by certain ion species. Chen [13] reported the first pinning of such defects in 4H-SiC using Cu implantation, where Cu was found to pin BPDs from expansion. Due to high energy requirements for Cu ion to penetrate thicker 4H-SiC epitaxial layers for application in higher voltage class, Kato [14, 15] recently demonstrated that the deep implantation of protons in 4H-SiC at the buffer-substrate interface pins the stacking faults extending from substrate into drift layer and thus avoiding bipolar degradation. The mechanism suggested is that the carrier lifetime is reduced and thus stacking fault expansion is suppressed [16, 17]. The method is suitable for optimal suppression of SF when the implanted proton dose is >1E14 cm-2 and at the cost of additional ion species in the fabrication process.

In this study, Energy Filtered Ion Implantation (EFII) technology was employed to implant 0-19 MeV equivalent energies of nitrogen in one step to improve the material property significantly by making the material defects such as 1SSF and Partial Dislocations (PD) dormant to recombination enhanced dislocation glide in one process step. At the same time, EFII also offers custom specific drift zone doping, with superior precision control on doping homogeneity from batch to batch and wafer to wafer in mass production [18].

Experimental Approach

To study the influence of suppressing 1SSF expansion in commercially available 4H-SiC material using EFII technology, optical stressing was employed [19–21]. This technique visualizes/reveals any nucleation sites or potential killer defects present in the epitaxial layer with UV excitation which are not usually detectable with conventional photoluminescence scan. In our experiments, we examined commercial epitaxial wafers from different vendors, by varying parameters such as Nitrogen implant concentration, epitaxial layer thickness, and taking into account defect correlation before and after EFII process.

Approach 1: Nominally un-doped 4H-SiC epitaxial wafers with a 5 μm thick epitaxial layer and a 0.5 μm buffer layer were used to study defect correlations across different regions on the wafer under varying implant concentrations. 19 MeV Nitrogen ions were implanted on three wafers (A, B, C) using EFII Technology. Wafers A and B were implanted identically in each quadrant with concentrations between 1E15 and 1E16 cm-3, while Wafer C was implanted with a lower concentration range of 1E14 to 1E15 cm-3. The implantation depth was 8.35 μm, which extended beyond the epitaxial layer into the substrate. Followed by 1700°C dopant activation annealing for 30 minutes in Ar ambient. Wafer description and implant parameters are detailed in Table 1 illustrated in Fig. 1. UV stressing conditions are described further.

Table 1: Description of wafer properties with N epitaxy and region of implanted concentrations of 19 MeV Nitrogen with EFII technology on the wafers.

Wafer label	BPD density* [cm^{-2}]	Epitaxial concentration [cm^{-3}]	Epitaxial thickness [μm]	Implanted Nitrogen Concentration [cm^{-3}]			
				Quadrant 1	Quadrant 2	Quadrant 3	Quadrant 4
A	68	<5E14	5.01	1E+15	5E+15	No implant	1E+16
B	3	<5E14	5.17	1E+15	5E+15	No implant	1E+16
C	2	<5E14	5.04	5E+14	1E+14	No implant	1E+15
D	80	5E+15	8.05	5E+15			

*Claimed by wafer vendor

Approach 2: A wafer from a different vendor, with an 8 μm epitaxial layer and 5E15 cm-3 nitrogen doping concentration, was analyzed for 1SSF expansion under 72 Wcm-2 UV stressing before and after the EFII process. This means the non-implanted wafer initially was UV stressed, density of expanded 1SSF defects were measured, then annealed at 800°C for 1 hour to contract (remove) the defects[19]. After implantation with 19 MeV Nitrogen using EFII technology and subsequent activation annealing, the same positions were UV stressed again to observe changes in 1SSF expansion density.

Details of the UV stress tests are described in the Table 2. We have estimated, that these intensities correspond to an electrical current density in the range 900-2000 Acm-2 for 72 Wcm-2 and 142 Wcm-2 from formula provided in [21] considering the highest surface recombination velocity (for k=0.03, So=10000) and correlating the results from other studies [22–24]. However, direct correlation of UV

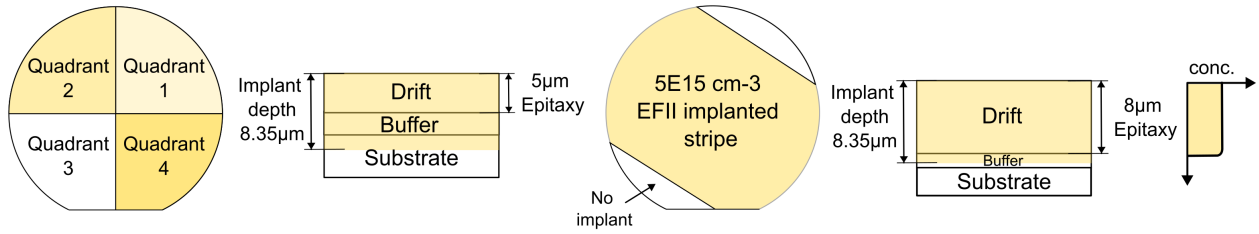

Fig. 1: Illustration of implanted regions on Wafer A,B,C *left* and Wafer D *right* with EFII Technology corresponding to the data as mentioned in Table. 1

intensity to electrical current density is still in discussion [20, 21]. Comparing this study to earlier optical UV stress intensities, it can be considered that the epitaxial layers are under high UV stress conditions.

Table 2: Summary of UV illumination stress experiments done on the wafers with test areas of size 10x10mm.

UV Source	UV Intensity [Wcm^{-2}]	Illumination time [s]	Illuminated wafers
Nd-YAG (355 nm)	72	2000	A, B, D
Nd-YAG (355 nm)	142	4000	A, B, C

Carrier lifetime measurements were performed on these EFII implanted regions to study the mechanism of pinning BPD/PD from expanding. µ-PCD measurements with 349 nm laser source and channel frequency of 26 GHz was used for wafer maps of A, B and C. For Wafer D, single point measurements at implanted and non implanted region were performed with µ-PCD with YAG266 nm as the excitation source and channel frequency of 10 GHz and compared to its Time Resolved Photoluminescence (TRPL) measurements. [14].

Results and Discussions

Approach 1 The UV stressing with an intensity of 72 Wcm-2 did not reveal any expanded 1SSF at any positions on wafers A and B. This could be due to the threshold density of carrier concentrations necessary for 1SSF expansion was not met in these 5µm thin layer [25]. However, after UV stressing with 142 Wcm-2, Fig. 2 shows the density of expanded 1SSF in no implant region, compared to EFII implanted regions at all test locations for wafer A, B and C. In Wafer A, a significantly higher density of the expanded 1SSF defects in no implant region is observed in contrast to the EFII implanted regions at all test positions. In case of Wafer B, there was only expansion of 1SSF in the non implanted region and no signature of 1SSF in any of the EFII implanted quadrants except negligible change around triangular defects was detected. On the other hand, Wafer C (where the implant concentrations were $\leq$1E15 cm-3) revealed that there were expanded 1SSF both in non implanted region and EFII implanted region but the difference being the density was lower compared to the no implant region.

Approach 2 Photoluminescence (PL) images of the defect behavior from wafer D is summarized in Fig.3. All test regions illuminated with UV are 10x10 mm in size. Region 1 was a random location on the wafer. At selected positions in this region, there were no 1SSF/BPD/PD observed at 420 nm and >700 nm on as-grown epitaxial material before UV stressing. Many expanded 1SSF were detected after UV stressing with 72 W/cm-2. The nucleation sites for these expanded defects were previously undetected. Fabrication of devices at such locations result in device degradation. These

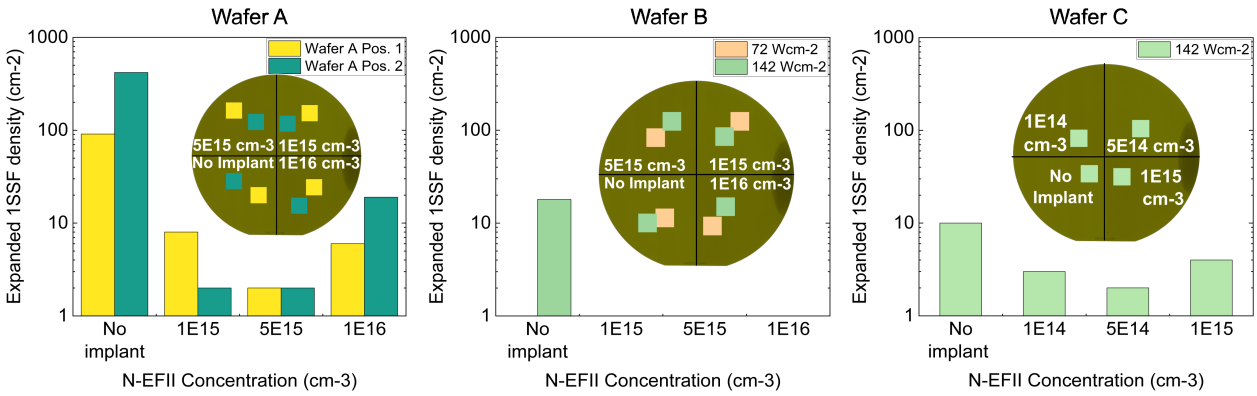

Fig. 2: Measured density of expanded 1SSF density on wafer A, B and C corresponding to EFII implant concentration at positions of area 10x10mm as illustrated *(inset)* for each wafer.

are considered to be the BPD-TED conversion points. However after contracting these expanded 1SSF with 800°C anneal for 1 hour, EFII implantation with activation annealing was performed. To observe the effect of EFII on nucleation sites, UV stress was repeated under the same conditions as before. The PL images reveal that EFII process made significant number of these nucleation sites immune to REDG in contrast to earlier observation.

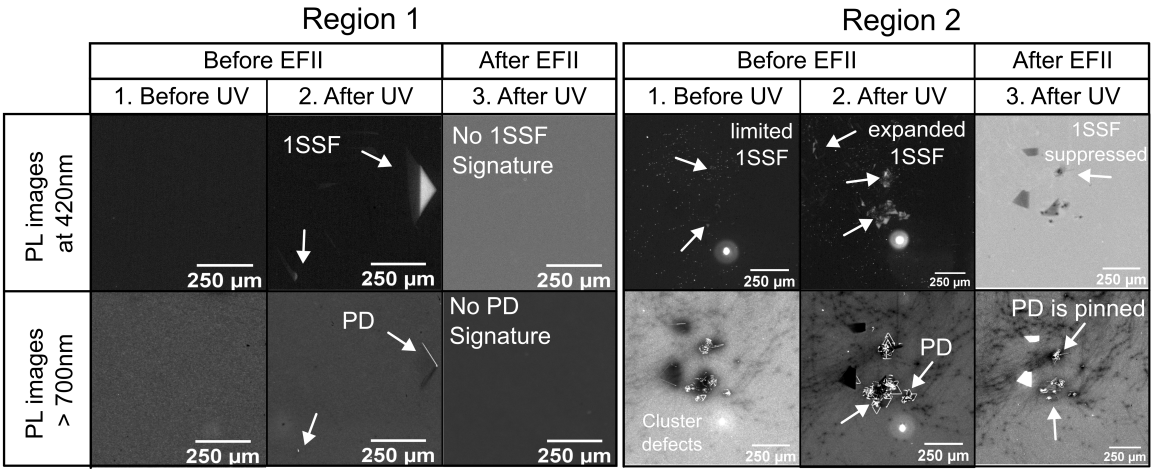

Fig. 3: PL images from wafer D reveal, previously undetected nucleation sites which expand after UV stress on as-grown material were successfully suppressed from expanding into 1SSF after the EFII process, as observed in both 420nm, >700nm images corresponding to 1SSF and PD respectively. On region 2, PL images of cluster defects demonstrates the extent to which EFII restricts the movement of mobile PDs from nucleation sites in all lateral crystal directions, even under identical stress conditions.

On region 2, (which is a cluster defect) the extent of PD (bright lines in >700 nm PL images after UV stress corresponding to 1SSF in 420 nm image) expansion length shows that for same stressing conditions the material is less susceptible to dislocation glide. In Fig. 4(a), the implantation profile of Nitrogen can be seen extending into the buffer layer at 8.35µm measured with SIMS and in Fig. 4(b) the total density of expanded 1SSF before and after the EFII process at these two regions are compared. Hence, it is evident that in all the wafers the trend remains similar. The expanded density of 1SSF corresponding to Nitrogen implanted regions with EFII, irrespective of epitaxial layer thickness show immunity to REDG to a significant extent. The summary of these results are exhibited in Fig. 6(a) excluding cluster defect data for a fair comparison of usable wafer regions in power device manufacturing.

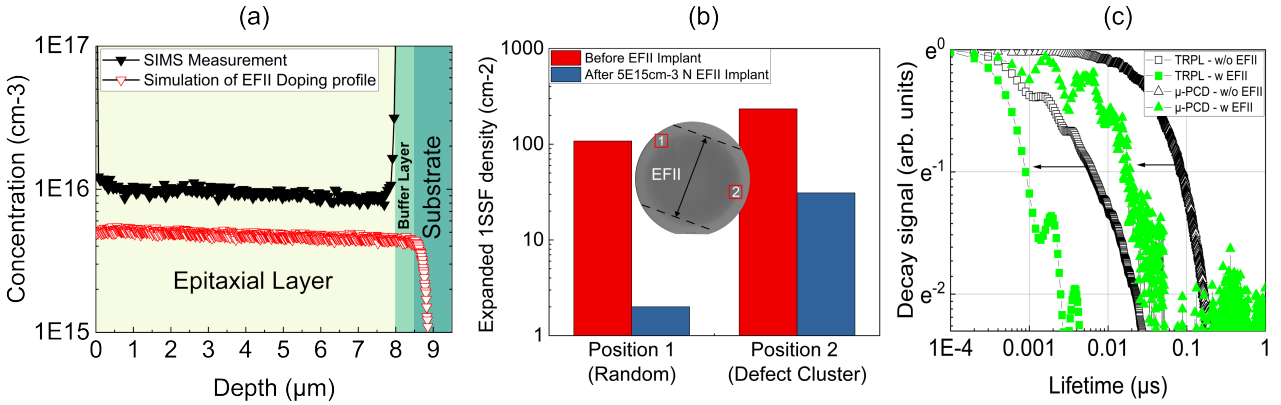

Fig. 4: (a) Illustration of implantation depth with EFII using GEANT4 simulation and SIMS measurement showing the Nitrogen profile on wafer D. (b) Significant reduction in density of expanded 1SSF witnessed before and after EFII process at both the regions. (c) Carrier life-time measurements with both TRPL and μ-PCD is compared on 8 μm epitaxial layer at test points with EFII and without EFII locations. It is observed that the lifetime is decreased from 77.2 to 23.8 ns after EFII process which implanted 5E15 cm-3 N over an existing 5E15 cm-3 N concentration.

Carrier lifetime measurements: μ-PCD measurements done on wafer A, B and C reveal that the regions with higher concentrations >5E15 cm-3 of Nitrogen implanted with EFII reduced the carrier lifetime values lower than the non-implanted region mapped in Fig. 5 which remains valid for reduction of life-time as a mechanism that suppresses 1SSF expansion from previous studies. This is also evident in Wafer D which was measured with TRPL and μ-PCD at two points (with EFII and without EFII) shown in Fig.4 (c). Carrier lifetimes in the un-implanted regions of Wafer D and the EFII-implanted regions of Wafer A and B (with a total N concentration of 5E15 cm-3) were found to be similar, approximately 70-80 ns. The results indicate that the carrier lifetime is primarily influenced by factors other than the presence of implanted nitrogen at the given concentration. This suggests that the implantation process itself did not significantly alter the carrier lifetime in the regions compared. However, at lower concentrations ≤1E15 cm-3, the carrier lifetime is slightly *higher* than in non implanted region and yet effective suppression of 1SSF is observed, where the mechanism is not well understood. The lifetime corresponding to implanted nitrogen concentrations are summarized in Fig. 6(b).

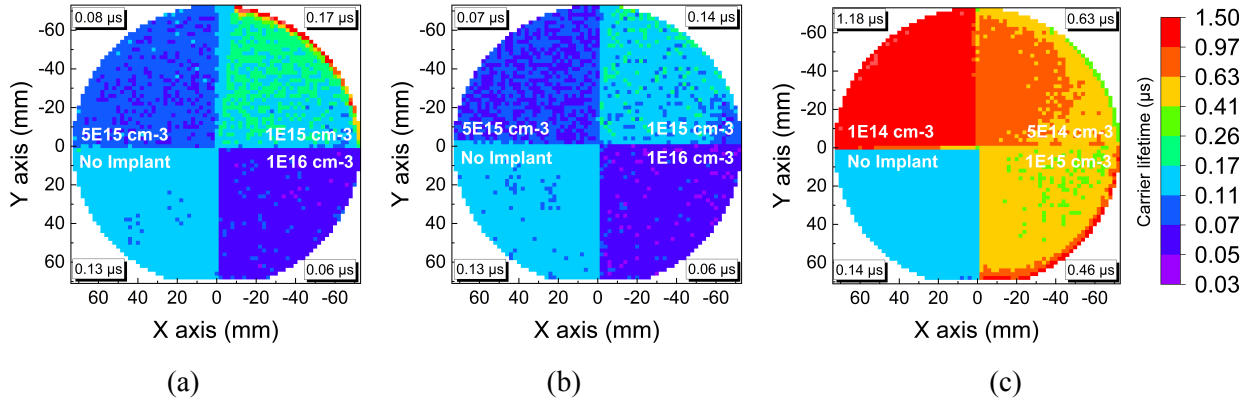

(a) (b) (c)

Fig. 5: Carrier lifetime maps of 5 μm thick epitaxial layer on Wafer A (a), Wafer B (b) and Wafer C (c) were measured with μ-PCD (with 3 mm edge exclusion) after the UV illumination tests. It is witnessed that at lower implant concentration the lifetime apparently improves provided the material is also having lower intrinsic defect density. Median values of the quadrants with implanted N+ concentrations are labeled inset.

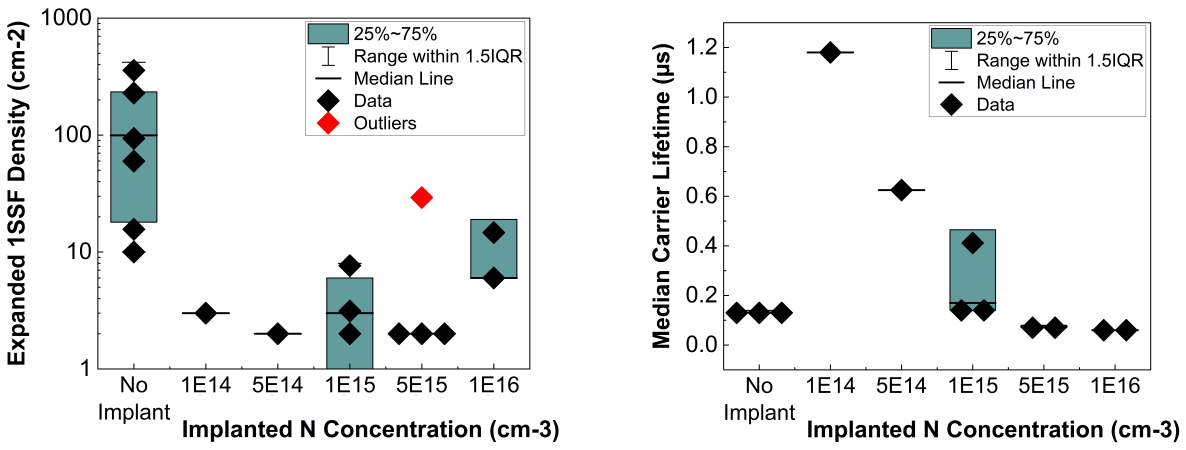

(a) (b)

Fig. 6: Expanded 1SSF defect density vs implanted nitrogen concentration, excluding cluster defects. EFII-implanted regions showed 10 times fewer defects than non-implanted areas. (b) Carrier lifetime vs implanted nitrogen concentration, improved by 10 times at the lowest concentration and decreased exponentially with increasing concentration, influenced by intrinsic material properties.

We expect that the improvement in carrier lifetime is related to Nitrogen atoms preferentially filling carbon vacancies making the material more useful, similar to carbon implantation [26, 27]. Hence, carrier lifetime reduction mechanism is considered to be one of the contributing factor to the suppression of stacking fault expansion.

Lattice work hardening seems to be the other contributing factor that could getter the defects from expanding by introduction of Nitrogen atoms in implanted material increasing the critically resolved shear stress (CRSS) in SiC matrix [14, 28–30]. The exact mechanism that significantly contributes to the pinning effect of these glide planes is yet to be studied, careful deep level transient spectroscopy (DLTS) measurements compared with PL spectrum data could reveal more information on how the defects (V_{Si}, V_C, Si_i ,C_i) caused by ion implantation that interact with recombination centers or trap levels that hinders the dislocation glide.

Summary

Demonstration of Nitrogen implantation using EFII technology to effectively suppresses the recombination enhanced dislocation glide (REDG) of 1SSF is shown. These results indicate approximately 10 times lower defect concentration expanded in implanted regions compared to non-implanted areas for concentration range between 1E14-1E16 cm-3. Furthermore, significant improvement in carrier lifetime is observed in the as grown 4H-SiC epitaxial material following the EFII process at lower concentrations below 1E15 cm-3. These findings suggest that REDG is influenced not only by a reduction in carrier lifetime but also by complex recombination mechanism involving the interaction between implanted defects and pre-existing recombination centers, warranting further investigation. Thus, a single EFII processing step not only enables the achievement of a highly homogeneous doping profile in SiC epitaxial layers but also enhances the material's resistance to bipolar degradation, outperforming as-grown epitaxial layers.

Acknowledgements

All the ion implantations were conducted at the Ion Beam Center (IBC) of Helmoltz-Zentrum Dresden-Rossendorf (HZDR). The standard dopant activation annealing was performed at Fraunhofer-Institut für Integrierte Systeme und Bauelementetechnologie (IISB), Erlangen.

References

[1] Victor Veliadis. "SiC Mass Commercialization: Present Status and Barriers to Overcome". In: *Materials Science Forum* 1062 (2022), pp. 125–130.

[2] Tsunenobu Kimoto and James A. Cooper. *Fundamentals of silicon carbide technology: Growth, characterization, devices and applications*. Singapore: John Wiley & Sons Singapore Pte. Ltd, 2014.

[3] Peder Bergman et al. "Crystal Defects as Source of Anomalous Forward Voltage Increase of 4H-SiC Diodes". In: *Materials Science Forum* 353-356 (2001), pp. 299–302.

[4] Anant Agarwal et al. "A New Degradation Mechanism in High-Voltage SiC Power MOSFETs". In: *IEEE Electron Device Letters* 28.7 (2007), pp. 587–589.

[5] Z. Zhang and T. S. Sudarshan. "Basal plane dislocation-free epitaxy of silicon carbide". In: *Applied Physics Letters* 87.15 (2005).

[6] Z. Zhang, E. Moulton, and T. S. Sudarshan. "Mechanism of eliminating basal plane dislocations in SiC thin films by epitaxy on an etched substrate". In: *Applied Physics Letters* 89.8 (2006).

[7] Naoyuki Kawabata et al. "Effects of Basal Plane Dislocation Density in 4H-SiC Substrate on Degradation of Body-Diode Forward Voltage". In: *Silicon Carbide and Related Materials 2015*. Vol. 858. Materials Science Forum. Trans Tech Publications Ltd, June 2016, pp. 384–388.

[8] M. Skowronski et al. "Recombination-enhanced defect motion in forward-biased 4H–SiC p-n diodes". In: *Journal of Applied Physics* 92.8 (2002), pp. 4699–4704.

[9] A. Galeckas, J. Linnros, and P. Pirouz. "Recombination-induced stacking faults: evidence for a general mechanism in hexagonal SiC". In: *Physical Review Letters* 96.2 (2006), p. 025502.

[10] Shohei Hayashi et al. "Influence of basal-plane dislocation structures on expansion of single Shockley-type stacking faults in forward-current degradation of 4H-SiC p–i–n diodes". In: *Japanese Journal of Applied Physics* 57.4S (2018), 04FR07.

[11] Masashi Kato et al. "Observation of carrier recombination in single Shockley stacking faults and at partial dislocations in 4H-SiC". In: *Journal of Applied Physics* 124.9 (2018).

[12] Yi Chen et al. "Interaction between Recombination Enhanced Dislocation Glide Process Activated Basal Stacking Faults and Threading Dislocations in 4H-Silicon Carbide Epitaxial Layers". In: *MRS Proceedings* 994 (2007).

[13] Bin Chen et al. "Pinning of recombination-enhanced dislocation motion in 4H–SiC: Role of Cu and EH1 complex". In: *Applied Physics Letters* 96.21 (2010).

[14] Masashi Kato et al. "Suppression of stacking-fault expansion in 4H-SiC PiN diodes using proton implantation to solve bipolar degradation". In: *Scientific reports* 12.1 (2022), p. 18790.

[15] Shunta Harada et al. "Suppression of stacking fault expansion in a 4H-SiC epitaxial layer by proton irradiation". In: *Scientific reports* 12.1 (2022), p. 13542.

[16] T. Tawara et al. "Short minority carrier lifetimes in highly nitrogen-doped 4H-SiC epilayers for suppression of the stacking fault formation in PiN diodes". In: *Journal of Applied Physics* 120.11 (2016).

[17] Toshiki Mii et al. "Analysis of carrier lifetime in a drift layer of 1.2-kV class 4H–SiC devices toward complete suppression of bipolar degradation". In: *Materials Science in Semiconductor Processing* 153 (2023), p. 107126.

[18] Constantin Csato et al. "Energy filter for tailoring depth profiles in semiconductor doping application". In: *Nuclear Instruments and Methods in Physics Research Section B: Beam Interactions with Materials and Atoms* 365 (2015), pp. 182–186.

[19] Kazumi Takano and Yasuyuki Igarashi. "Effective Method (Selective E-V-C Technique) to Screen out the BPDs that Cause Reliability Degradation". In: *Materials Science Forum* 1062 (2022), pp. 273–277.

[20] Kazumi Takano et al. “Accuracy of EVC Method for the PiN Diode Pattern on SiC Epi-Wafer”. In: *Defect and Diffusion Forum* 434 (Aug. 2024), pp. 15–21.
[21] Yasuyuki Igarashi et al. “Study on Quantification of Correlation between Current Density and UV Irradiation Intensity, Leading to Bar Shaped 1SSF Expansion”. In: *Defect and Diffusion Forum* 434 (Aug. 2024), pp. 23–31.
[22] A. Iijima and T. Kimoto. “Estimation of the critical condition for expansion/contraction of single Shockley stacking faults in 4H-SiC PiN diodes”. In: *Applied Physics Letters* 116.9 (2020).
[23] Kazuya Konishi et al. “Stacking fault expansion from basal plane dislocations converted into threading edge dislocations in 4H-SiC epilayers under high current stress”. In: *Journal of Applied Physics* 114.1 (2013).
[24] Junji Senzaki et al. “Challenges to realize highly reliable SiC power devices: From the current status and issues of SiC wafers”. In: IEEE, 2018.
[25] T. Tawara et al. “Injected carrier concentration dependence of the expansion of single Shockley-type stacking faults in 4H-SiC PiN diodes”. In: *Journal of Applied Physics* 123.2 (2018).
[26] Liutauras Storasta and Hidekazu Tsuchida. “Reduction of traps and improvement of carrier lifetime in 4H-SiC epilayers by ion implantation”. In: *Applied Physics Letters* 90.6 (2007).
[27] Tetsuya Miyazawa and Hidekazu Tsuchida. “Point defect reduction and carrier lifetime improvement of Si- and C-face 4H-SiC epilayers”. In: *Journal of Applied Physics* 113.8 (Feb. 2013), p. 083714.
[28] S. McGuigan et al. “Effects of indium lattice hardening upon the growth and structural properties of large□diameter, semi□insulating GaAs crystals”. In: *Applied Physics Letters* 48.20 (May 1986), pp. 1377–1379.
[29] P. Budzynski et al. “Effect of mixed N and Ar implantation on tribological properties of tool steel”. In: *Vacuum* 78.2-4 (2005), pp. 685–692.
[30] D. González et al. “Work-hardening effects in the lattice relaxation of single layer heterostructures”. In: *Applied Physics Letters* 71.17 (1997), pp. 2475–2477.